

Received July 21, 2020; reviewed; accepted August 26, 2020

Commercial sponges in heterogeneous catalysis: developing novel composites with cobalt and silver

Sonia Żółtowska ¹, Martyna Modelska ¹, Adam Piasecki ², Teofil Jesionowski ¹

¹ Institute of Chemical Technology and Engineering, Faculty of Chemical Technology, Poznan University of Technology, Berdychowo 4, PL-60965 Poznan, Poland

² Institute of Material Engineering, Faculty of Material Engineering and Technical Physics, Poznan University of Technology, Jana Pawla II 24, PL-60965 Poznan, Poland

Corresponding author: Teofil.Jesionowski@put.poznan.pl (Teofil Jesionowski)

Abstract: The use of commercial sponges in materials science has gained much recent attention. Their unique properties, namely a fibrous, rigid skeleton, thermal stability and resistance to acid and basic hydrolysis, have been the primary motivation to use them in the development of new composites. In this work, a simple method of immobilization of cobalt and silver cations, followed by their reduction using sodium borohydride, was successfully applied for the first time to obtain functionalized spongin scaffolds. Three different materials, labeled Co_spongin, Ag_spongin and Co-Ag_spongin, were prepared. Their morphological and physicochemical properties were explored using various techniques (SEM+EDS, TG/DTA, FTIR). The focal point of the research was the application of the resulting materials in the reaction of 4-nitrophenol reduction with sodium borohydride in water. It was found that all of the composites possess superior activity in the reduction of 4-nitrophenol, achieving high rate constants of 0.31 min⁻¹ for Ag_spongin, 0.52 min⁻¹ for Co_spongin and 0.86 min⁻¹ for Co-Ag_spongin. Reusability tests showed that all of the composites could be reused five times. Additional structural analysis after catalytic application showed no visible changes in the morphology of the catalysts. The results indicate that spongin can be considered as a facile, cost-effective, renewable and environmentally friendly three-dimensional support for use in heterogeneous catalysis.

Keywords: commercial sponge, biomimetic, 4-nitrophenol, cobalt, silver

1. Introduction

Sponges (phylum Porifera), being among the world's oldest and simplest animals, are currently the subject of intensive investigation (Boury-Esnault et al., 2013). Especially commonly studied are representatives of the class Demospongiae, due to their characteristic fibrous skeletons built from chitin or spongin as the main organic component. Spongin is a fascinating protein with a still unknown chemical structure, although it contains the same amino acids already described in collagen and keratin. Their presence is responsible for the rigid framework of the sponge skeleton, which creates an extraordinary system of anastomosed open-porous channels (Ehrlich et al., 2003; Pallela et al., 2011). This unique dendritic structure enhances the mechanical properties of the sponge skeleton.

Additionally, the chemical and thermal stability of spongin are similar to those of keratin, which means that spongin is resistant to mild acid and basic hydrolysis and enzymatic treatment, and it is thermally stable up to 150 °C (Jesionowski et al., 2018). Moreover, the development of marine ranching methods for the cultivation of spongin-based sponges as commercial products makes them a novel, renewable source of naturally prefabricated three-dimensional proteinaceous scaffolds with promising applications in materials science (Jesionowski et al., 2018). However, it is important to understand the difference between the commonly used terms: *sponge*, *sponge skeleton* and *commercial sponge*. According to Jesionowski et al. (2018), the term *sponge* refers to the whole organism: body and skeleton. The *skeleton*

is the cell-free, demineralized and depigmented skeletal construct, while *commercial sponge* refers to a sponge skeleton built from spongin. These commercial sponges are the main source for the sponge industry (Jesionowski et al., 2018).

Due to the aforementioned structural, chemical and mechanical properties, spongin matrices from various representatives of Demospongiae are currently under examination for purposes of tissue engineering (Green et al., 2003), biomimetics and Extreme Biomimetics (Szatkowski and Jesionowski 2017; Szatkowski et al., 2015, 2017, 2018). As an example, Szatkowski et al. synthesized two different hybrid materials with spongin, namely spongin-hematite (Szatkowski et al., 2015) and spongin-TiO₂ (Szatkowski and Jesionowski 2017; Szatkowski et al., 2017). As a result, both inorganic phases entirely covered the spongin fibers, which indicated the high affinity of spongin towards iron oxide and titanium dioxide. The spongin-TiO₂ composite possessed good photocatalytic ability towards methylene blue dye, achieving a good yield of degradation. On the other hand, the spongin-hematite composite was utilized as an anode material in a capacitor, with satisfactory results.

Commercial sponges have also been successfully applied as a support for enzyme immobilization (Zdarta et al., 2017). Moreover, evaluation of the ability of spongin to adsorb various dyes has led to the development of unique hybrid materials with antibacterial (Norman et al., 2016a), antiradical (Norman et al., 2016b) and photocatalytic properties. For example, spongin-iron phthalocyanine (Norman et al., 2018) and spongin-copper phthalocyanine (Norman et al., 2016c) composites exhibited excellent activity in the degradation of Rhodamine B and of phenol and its halogenated derivatives. Both studies showed that spongin acts as an active support with weak photocatalytic activity, which can be significantly enhanced after successful immobilization of the dye. Recently, the carbonization of spongin has been developed (Petrenko et al., 2019; Szatkowski et al., 2018) as a method to produce fibrous, sponge-like carbon materials which can be applied as a component of advanced MnO₂-carbon and Cu/Cu₂O-carbon composites with electrochemical properties (Szatkowski et al., 2019) or with catalytic activity in the reduction of 4-nitrophenol (Petrenko et al., 2019).

It appears from the studies mentioned above that the most attention has been paid to the formation of photocatalysts or electrochemically active materials derived from spongin. Therefore, the motivation of this work was the development, for the first time, of composites based on spongin as a support for cobalt and silver particles, using a simple method of immobilization and reduction of adsorbed metal cations, followed by their utilization as heterogeneous catalysts in the reduction of 4-nitrophenol to 4-aminophenol in water. A kinetic evaluation and a reusability study were important milestones of this work. Our results show that by applying a simple method, a novel composite with superior catalytic performance can be developed.

2. Materials and methods

2.1. Materials

Specimens of the commercial marine sponge *Hippospongia communis* (Porifera: Demospongiae) were purchased from INTIB GmbH (Germany). Cobalt nitrate (CAS no. 10026-22-9) and silver nitrate (CAS no. 7761-88-8) were obtained from VWR (Germany), and 4-nitrophenol (CAS no. 100-02-7) and sodium borohydride (CAS no. 16940-66-2) were supplied by Sigma-Aldrich (Germany).

2.2. Purification and preparation of commercial sponge

The obtained commercial sponge skeletons were purified before functionalization to remove some foreign sand particles and calcium carbonate debris. The detailed purification methodology is described elsewhere (Norman et al., 2016ab). After cleaning, the commercial sponge skeletons were cut into pieces (4 cm × 4 cm × 4 cm) and subjected to the functionalization process.

2.3. Functionalization of commercial sponge

The functionalization process can be divided into two stages. The first stage was the immobilization of cobalt and silver ions on the commercial sponge. A piece of spongin (weight approximately 3 g) was placed in a conical flask and mixed with 100 cm³ of an aqueous solution of metal precursor: cobalt nitrate, silver nitrate, or a mixed solution of both precursors consisting of 50 cm³ Co(NO₃)₂ and 50 cm³

AgNO₃. The concentration of silver and cobalt salt was 5 g/dm³. This mixture was shaken in a thermostated incubator (IKA Werke GmbH, Germany) for 60 minutes at temperature 25 °C. Then 50 cm³ of sodium borohydride solution (concentration 0.1 mol/dm³) was dosed directly into the mixture using a peristaltic pump at a rate of 1 cm³/min, followed by further shaking for an additional 60 min. Next, the product was filtered under reduced pressure, washed with ethanol three times and dried at 60 °C for 60 min. The immobilization and reduction procedure was repeated three times. After the third cycle, the prepared catalysts, labeled Co_spongin, Ag_spongin and Co-Ag_spongin, were subjected to ultrasonication treatment for 15 minutes and dried overnight at 60 °C.

2.4. Physicochemical and structural analysis

An EVO-40 microscope (Zeiss, Germany) was used to perform the scanning electron microscopy analysis. EDS X-ray microanalysis (Tescan, Czech Republic) was performed using Gamma-Tec instrumentation from Princeton Inc. (USA). Total reflection ATR-FTIR analysis was performed using Vertex apparatus (Bruker, Germany). Thermogravimetric analysis was carried out using the TGA/DTG method (Jupiter STA 449F3, Netzsch, Germany). Measurements were conducted under flowing nitrogen (20 cm³/min) at a heating rate of 10 °C/min over a temperature range of 25–1000 °C, with an initial sample weight of approximately 10 mg.

2.5. Catalytic tests

The model reduction reaction of 4-nitrophenol with sodium borohydride was used to determine the catalytic ability of the obtained hybrid materials. The reaction was performed in a 3 cm³ glass cuvette and monitored using a UV-Vis spectrophotometer (V-750 Jasco, Japan) in the wavelength range 250–500 nm. 2.5 cm³ of 4-nitrophenol solution at concentration 0.001 mol/dm³, 0.5 cm³ of 0.01 mol/dm³ solution of NaBH₄ and 5 mg of the tested hybrid material were placed in a quartz cuvette. The UV-Vis spectra were monitored every 1 min until the disappearance of the band characteristic for the 4-nitrophenol anion ($A_{max}=400$ nm). The reduction efficiency was calculated from the obtained spectra based on the calibration curve method.

Evaluation of the kinetics of 4-nitrophenol reduction was performed based on the zero-order and first-order kinetic models. Both of these models assumed a change in the concentration of 4-nitrophenol with time. The zero-order model is represented by the formula (1):

$$\frac{c_t}{c_0} = -k \cdot t \quad (1)$$

For the first-order model, the general equation is written as follows (2):

$$\ln \left(\frac{c_t}{c_0} \right) = \ln (C_0) - k \cdot t \quad (2)$$

where C_0 and C_t represent the concentration of 4-nitrophenol at the initial time and at time t respectively (mol/dm³), k denotes the rate constant (min⁻¹), and t is time (min). The rate constant is calculated from the slope of the corresponding plots.

The stability and reusability properties of the prepared hybrid materials were also evaluated. For this purpose, 5 mg of the catalyst was repeatedly used five times in catalytic cycles. After every run, the catalyst was separated from the reaction mixture, washed three times with water and ethanol, and dried for 30 min at 60 °C in a dryer. The effect of reuse of the prepared hybrid materials on their structural properties was also evaluated using scanning electron microscopy analysis.

3. Results and discussion

3.1. Physicochemical and structural analysis

A scanning electron microscope was used to investigate the effect of functionalization on the morphology and structure of the prepared spongin-based hybrid material. The SEM images obtained are shown in Fig. 1.

The structure and morphology of the commercial sponge skeleton are well described in previously published papers (Norman et al., 2016abc; Szatkowski et al., 2015). The characteristic, hierarchical structure of fibers consisting of fibrils which interweave with each other, typical of species of sea spon-

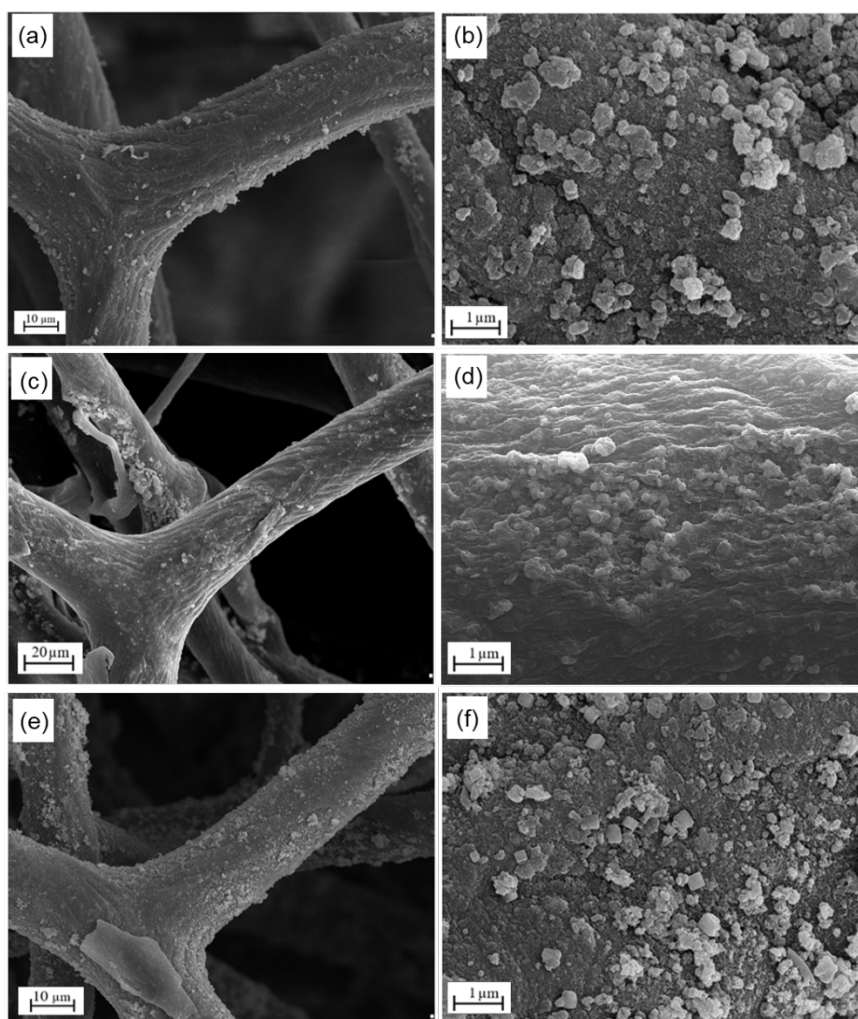


Fig. 1. SEM images of Co_spongini (a, b), Ag_spongini (c, d) and Co-Ag_spongini hybrid materials. Images at different magnifications

ges belonging to the subclass Keratosa, is observed. The SEM images obtained after functionalization with cobalt and silver show significant alterations (Fig. 1). From Fig. 1a and b it is visible that the fibrillar structure of spongini is covered with semi-spherical and semi-square structures, which has a tendency to agglomerate. The size of agglomerates varies, but does not exceed 2 μm . Similar structures are also present in the fibers depicted in Fig. 1e and f. Metallization with silver (Fig. 1c and d) results in a material in which the fibers are covered with small and spherical silver particles, which exhibit a lower tendency towards the formation of large agglomerates than is observed for the cobalt structures. The visible agglomerates are smaller than 1 μm . When a bimetallic system was prepared, structures representing both phases were observed on the fibers of the resulting material (Fig. 1e and f). A similar morphology of the metallic phase, corresponding to Co_3O_4 grains, was observed in a study by Allaedini and Muhammad (2013), where sodium borohydride was also applied in the synthesis of Co_3O_4 particles.

EDS mapping was carried out to investigate the chemical composition of the prepared hybrid materials (Fig. 2).

As shown in Fig. 1b–e, the fibers of the prepared materials are evenly covered with the cobalt or silver metallic phase. In the case of both solids, the surface content of Co or Ag is similar, at approx. 83 wt% (Fig. 2a). This indicates that spongini possesses similar affinity towards silver and cobalt. The difference in the content of oxygen between Co_spongini and Ag_spongini is insignificant. This result, together with knowledge of the Pourbaix diagram of cobalt and silver, suggests that for Co_spongini the metallic phase consists of cobalt and Co_3O_4 , while for Ag_spongini it consists mainly of the silver phase (Garcia et al., 2008; Hans et al., 2016). The presence of iodine, bromine, sulfur, iron and silica is related to the proteinaceous nature of the spongini skeleton; these elements were also found in previous studies

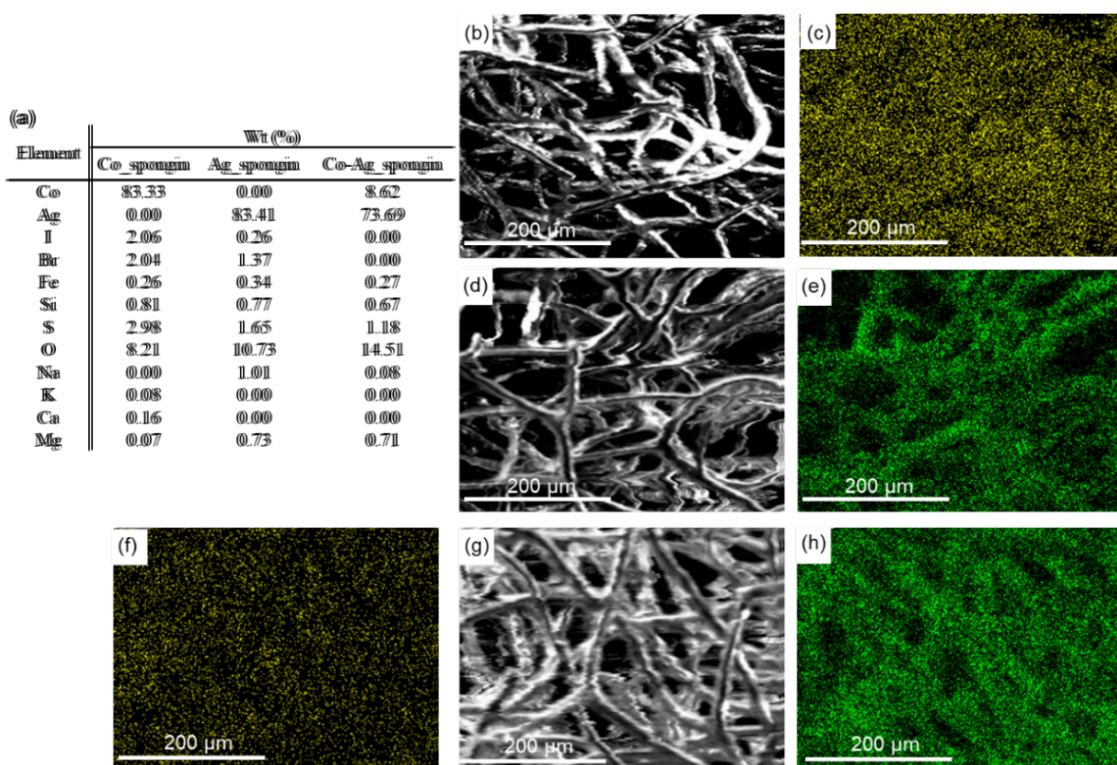


Fig. 2. Surface composition of the prepared hybrid materials (a); SEM image of Co_spongín (b) with Co mapping (c); SEM image of Ag_spongín (d) with Ag mapping (e); Co mapping of Co-Ag_spongín (f), its SEM image (g) and its Ag mapping (h)

(Jesionowski et al., 2018). The small amounts of calcium, magnesium and potassium can be explained by the marine origin of commercial sponge skeletons, and the small sodium content is derived from the reducer used during the synthesis. Surprisingly, for Co-Ag_spongín, the content of silver is much higher than that of cobalt. It seems that, when both cations are present during the synthesis, the spongín favorably binds silver. This is visible on the silver map, which shows fibers tightly covered by silver with the addition of cobalt.

TGA/DTA analysis was used to investigate the effect of heat on the samples. The plots obtained are shown in Fig. 3.

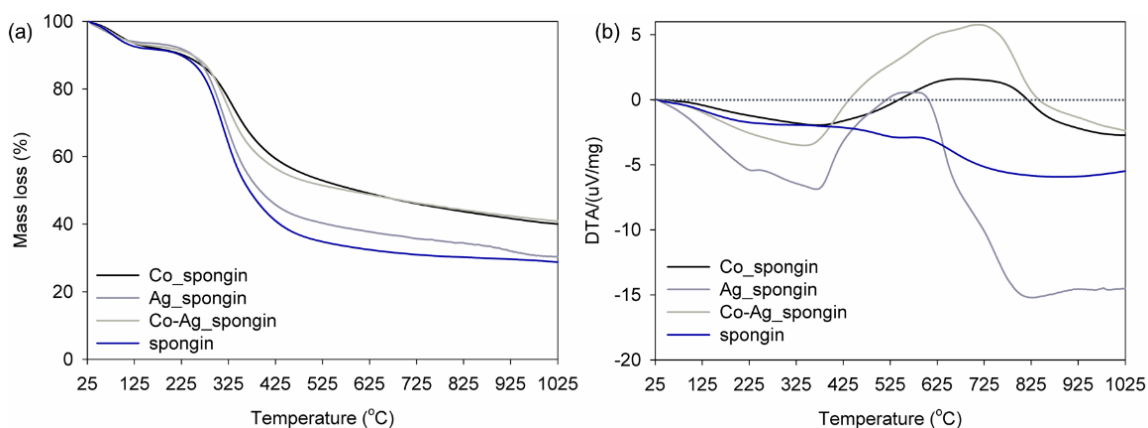


Fig. 3. TG (a) and DTA (b) plots obtained for spongín, Co_spongín, Ag_spongín and Co-Ag_spongín

In the case of spongín and all of the prepared composites, the TG curves exhibit two typical mass losses. The first occurred at a temperature of 130 °C (6% mass loss for all composites, 8% for spongín), being related to the evaporation of physically adsorbed water. The second mass loss, equal to 53.5% for Co_spongín, 65.5% for Ag_spongín, 53.1% for Co-Ag_spongín and 67% for spongín, occurred in the

temperature range 225–525 °C, and is attributed to the thermal decomposition of the spongin skeleton through the decomposition of protein bonds, disulfide bridges and hydrogen bonds. Interestingly, the thermal stability of all of the prepared materials is higher than for spongin itself, probably because the cobalt and silver particles control the thermal motion of the biopolymer matrix in the composite. This effect is especially prominent for the Co_spongin composite, which means that the presence of cobalt moieties enhances the thermal stability of the resulting material. Functionalization with silver does not have such a pronounced effect. The DTA plots revealed interesting features. For all examined samples, the first broad endothermic peak with a maximum at 330 °C can be associated with the evaporation of water and dehydroxylation of the spongin matrix. On the DTA plot for spongin, this peak is less strongly visible. The low intensity of endo/exo reactions observed for unmodified spongin may be associated with thermal inertia phenomena, which derive from the slow process of reaching equilibrium during the thermal treatment. The temperature of the second broad exothermic peak varies for different composites; it equaled 680 °C, 525 °C, 690 °C and 585 °C for Co_spongin, Ag_spongin, Co-Ag_spongin and spongin, respectively. This peak seems to be attributable to the release of methane, CH₄S and SO₂ from the spongin matrix together with thermal transformation of the metallic phase. The third broad endothermic peak with maximal temperature varying from 820 to 840 °C may be ascribed to the further release of SO₂ from the spongin matrix. Interestingly, combining silver and cobalt results in a rise in the transformation temperature and increases the intensity of this process.

With regard to the possible utilization of the prepared composites as catalysts, it is essential to investigate the chemical moieties located on the surface of the material. For this purpose, ATR-FTIR analysis was performed. The plots obtained are shown in Fig. 4.

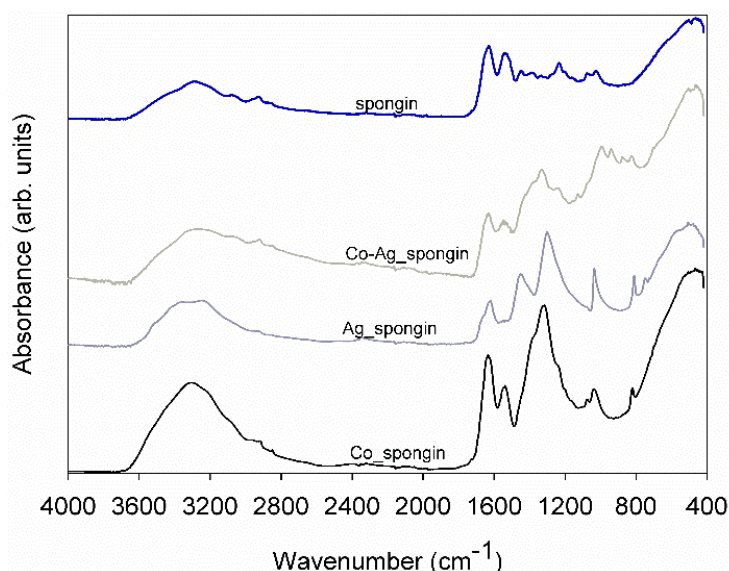


Fig. 4. ATR-FTIR spectra of Co_spongin, Ag_spongin and Co-Ag_spongin compared with the spectrum of unmodified spongin

The presented ATR-FTIR spectra exhibit some similarities with regard to the bands characteristic for spongin, whose FTIR spectrum is described in our previous work (Norman et al., 2016b; Szatkowski et al., 2017). A broad band in the wavenumber range 3300–3250 cm⁻¹ can be distinguished, characteristic for the overlapping stretching vibrations of N-H amide groups and O-H groups. Bands derived from aliphatic stretching vibrations of C-H groups, slightly visible in the range 3050–2990 cm⁻¹, overlap with a broad band corresponding to N-H and O-H groups. This is related to the existence of a hydrogen-bonded molecule of water, and it may be correlated with the presence of hydroxyl groups of cobalt oxide in the case of Co_spongin and Co-Ag_spongin. The peak in the range 1650–1610 cm⁻¹ derives from stretching vibrations of carbonyl groups. Interestingly, the wide band characteristic for stretching vibrations of CO-NH amide groups (1550–1450 cm⁻¹) is absent only for Ag_spongin. However, only for that material and pure spongin, a peak resulting from stretching vibrations of aromatic C_{ar}=C_{ar} structures is observed at 1450 cm⁻¹. The intense, broad band at 1340–1330 cm⁻¹ can be assigned to

in-plane bending vibrations of OH groups. There is also a band characteristic for stretching vibrations of C–O bonds in alcohols at 1050 cm^{-1} , not present in the spectrum of Co-Ag_spongin. The remaining signals in the range $1000\text{--}800\text{ cm}^{-1}$ can be ascribed to carbon moieties, especially C–C vibrations. The wide band in the range $540\text{--}530\text{ cm}^{-1}$ can be assigned to vibrations of C–S groups as well as C–Br and C–I halogen moieties. Due to strong overlapping, the Co–O vibrations for the samples Co_spongin and Co-Ag_spongin are not visible. It is important to note that the spongin surface is rich in carboxyl groups of amino acid residues, and peptide groups have a strong ability to bind silver and cobalt (Guo et al., 2011; Mandal et al., 2012). Notably, it is reported that amine groups from cysteine can easily bind silver particles. Therefore, the formation of bonds between cobalt and silver ions and amine groups from cysteine is considered as a primary mechanism of immobilization of these particles before chemical reduction.

3.2. Catalytic activity

To evaluate the catalytic ability of the prepared spongin-based composites, the reduction of 4-nitrophenol (4-NP) to 4-aminophenol (4-AP) using sodium borohydride in aqueous solution was carried out. This reaction is commonly applied to study the catalytic ability of metal particles (Noh and Meijboom 2014). The reduction of 4-nitrophenol to 4-aminophenol is thermodynamically possible ($E_{0|4\text{-NP}/4\text{-AP}} = -0.76\text{ V}$, $E_{0|\text{H}_3\text{BO}_3/\text{BH}_4} = -1.33\text{ V}$). However, this reaction does not take place without a catalyst due to kinetic barriers, principally the large difference in the potentials of the electron acceptor and donor. Therefore, the catalytic action of metal particles is related to the function of electronic relay systems, where electron transfer occurs from BH_4^- donor groups to nitro acceptor groups. As Fig. 5a illustrates, the addition of sodium borohydride leads to a red-shift of the absorption peak from 317 to 400 nm, and the formation of the 4-nitrophenolane anion by deprotonation. The addition of 5 mg of the prepared catalyst to the reaction system results in the initiation of the reduction reaction, which is visible from the decrease in the intensity of the peak characteristic for the 4-nitrophenolane anion, with a simultaneous increase in the intensity of the peak corresponding to 4-aminophenol ($A_{\text{max}} = 300\text{ nm}$). Finally, the total reduction of 4-nitrophenol leads to decolorization of the initial yellow-green solution (Fig. 5b).

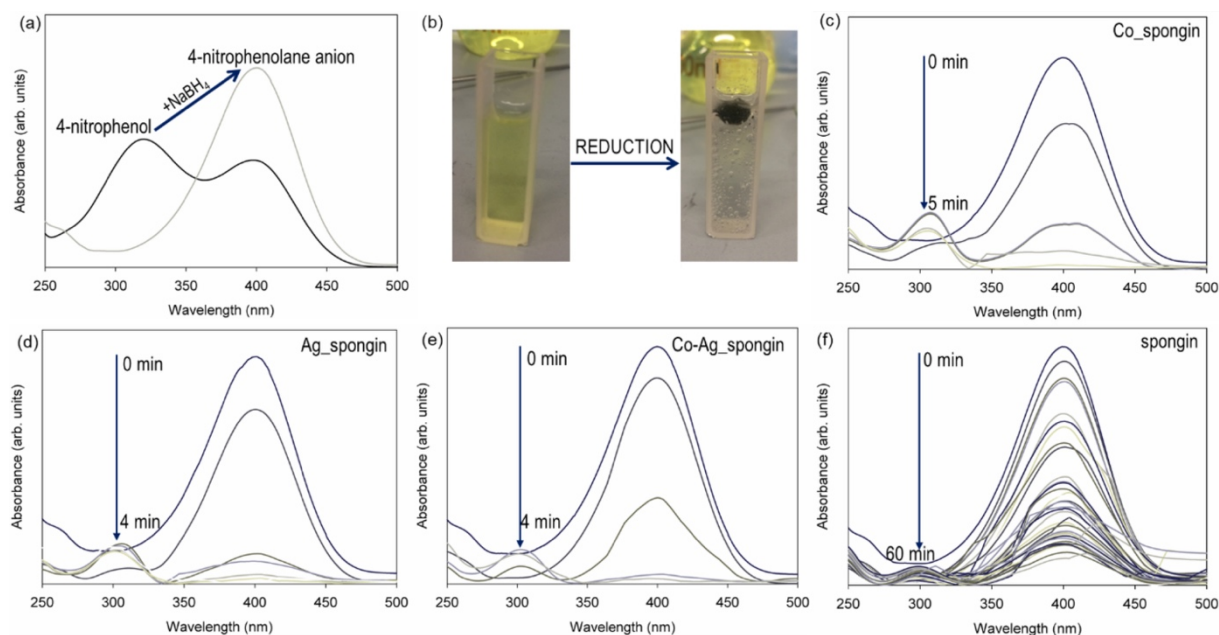


Fig. 5. UV-Vis spectra of 4-nitrophenol and 4-nitrophenolane anion (a); the reaction mixture before reaction (left) and after the reduction (right) (b); UV-Vis spectra of ongoing reduction of 4-nitrophenol after addition of NaBH_4 in the presence of Co_spongin (c), Ag_spongin (d), Co-Ag_spongin (e) and spongin (f)

Depending on the applied catalyst, after 5 min (Co_spongin) or 4 min (Ag_spongin and Co-Ag_spongin) the peak characteristic for the 4-nitrophenolane anion disappeared, indicating the end

of the reduction, which signifies 100% reduction efficiency. The shape of the spectra provides evidence that the 4-NP is gradually reduced and no additional products are formed during the reaction. It is important to note that the reduction reaction starts immediately after the introduction of the catalyst. This means that the induction period—described elsewhere (Gao et al., 2007; Pich et al., 2006) as a common issue when heterogeneous metallic catalysts are used—is not observed in our study. The absence of an induction period seems to be related to the fibrous structure with an interconnected microporous network, which provides satisfactory diffusion of substrates towards the surface of the catalyst. Besides, the size of the metallic phase also plays an important role and affects the presence of an induction period. In the case of the presented materials, the size of metallic grains does not exceed 2 μm ; however, good dispersion of the metallic particles on the spongin fibers results in easy access to their surface and counteracts the negative effect of the large size of the grains (Kuroda, Ishida, and Haruta 2009). The same reaction was also carried out in the presence of 5 mg of pure spongin skeleton (Fig. 5f). Surprisingly after 60 minutes of reaction, the reduction efficiency was 65%. The formation of 4-aminophenol is confirmed by the presence of its characteristic absorbance peak. In this case also, no induction period is observed. This extraordinary catalytic ability may be linked to the chemical composition of spongin. The various functional groups, especially hydroxyl and amide, present in the structure of this material can enhance the sorption properties of reagents, and can also act as an electron relay system. However, such a long reaction time excludes the application of pure spongin as a catalyst. These results prove that functionalization with cobalt and silver leads to significant enhancement of catalytic ability, due to the formation of an effective electron relay system or by the catalytic activity of the metallic phases towards hydrogen evolution from NaBH_4 ; therefore, the enhanced catalytic properties of the prepared composites are prominent (Garron et al., 2009). In addition, it is concluded that spongin can assist in the sorption of reagents and electron transfer. Thus, it can play the role of an “active support”. In the next step, the kinetic parameters of reduction were evaluated. According to the chemistry of this reaction, two models were considered: zero-order and first-order. The obtained rate constants and correlation coefficients are given in Table 2.

Table 2. Kinetic parameters calculated for the reduction of 4-nitrophenol using various catalysts

Catalyst	Zero-order model		First-order model	
	k (min^{-1})	R ²	k (min^{-1})	R ²
Co_spongin	0.09	0.971	0.52	0.994
Ag_spongin	0.04	0.975	0.33	0.945
Co-Ag_spongin	0.31	0.958	0.86	0.980

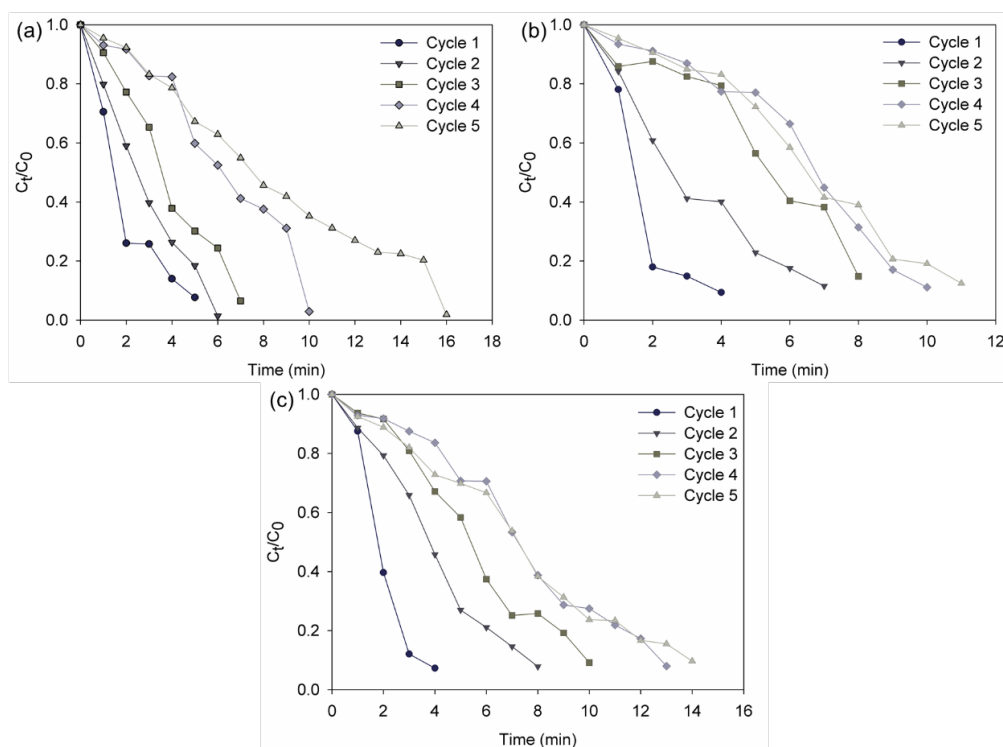
It is apparent that good linear correlation was obtained using the first-order model. Because the initial concentration of sodium borohydride was much higher than that of 4-nitrophenol, it can be assumed to be constant. Therefore, the model is called pseudo-first-order. Surprisingly, the lowest rate constant (independently of the model used) was obtained for Ag_spongin, even when the reduction of 4-nitrophenol using Co_spongin as catalyst lasted one minute longer. This result can be explained by the faster changes in concentration of 4-nitrophenol using the Co catalyst, and therefore, independently of reaction time, the calculated rate constant is higher. Some literature results provide evidence that strong interactions between the support and metal particles can hamper the reduction efficiency and negatively influence the rate of reduction (Liu, Yang, and Huang 2006; Liu, Yang, and Xie 2007). This suggests that the interaction between silver and cysteine groups, which is well documented, may negatively influence the catalytic ability of the Ag_spongin material. Not without significance is the fact that the highest rate constant was computed for the Co-Ag_spongin composite. This finding provides evidence that the combination of two metallic phases results in a more efficient catalyst, where the two phases act synergistically in the electron transport from the borohydride anion to the 4-nitrophenol molecule. A comparison of the present results with those previously reported in the literature is shown in Table 3.

Table 3. Comparison of kinetic parameters of the reduction of 4-nitrophenol computed for various cobalt- and silver-based catalysts

Catalyst	Rate constant k	Source
Co_spongini	0.52 min ⁻¹	This work
Ag_spongini	0.33 min ⁻¹	
Co-Ag_spongini	0.82 min ⁻¹	
Ag nanoparticles stabilized by hydrogel	0.24 min ⁻¹	(Ai and Jiang 2013)
mesoporous Ag NPS/carbon composite	0.32 min ⁻¹	(Chi et al., 2014)
alloyed Cu/Ag NPs	0.23 min ⁻¹	(Wu et al., 2011)
Co doped CuO NPs	0.26 min ⁻¹	(Sharma et al., 2017)
Co ₂ P nanowires	0.09 min ⁻¹	(Huang, Wu, and Cheng 2017)

Nevertheless, the use of a renewable, three-dimensional support and the simple method of fabrication of spongini-based composites represent added value of the materials described here in comparison to other heterogeneous catalytic systems.

Critical properties essential for the success of any heterogeneous catalyst include its stability during repeated use and easy recovery from the reaction mixture. Thus, to evaluate the recycling properties of the prepared materials, the same catalyst was used repeatedly five times. After each run, the catalyst was washed with water and ethanol, and dried. Plots of C_t/C_0 versus time for each catalytic run are shown in Fig. 6.

Fig. 6. Plots of C_t/C_0 versus time for Co_spongini (a), Ag_spongini (b) and Co-Ag_spongini (c)

It is apparent from Fig. 6a-c that for all tested catalysts the time of reaction increases with repeated use. The smallest increase in time is observed for the Ag_spongini catalyst. For the Co-Ag_spongini composite, the increase in reaction time is more significant than for Ag_spongini, but smaller than for Co_spongini. However, to decide whether the addition of cobalt has a negative influence on the stability of the prepared composites, kinetic parameters must be calculated for each catalyst. In Table 4, the rate constants calculated from the pseudo-first-order model are compared.

The rate constants calculated for the Co-Ag_spongini composite is high only in the first and second cycle. Subsequently, a gradual decrease in the value of the k parameter for this catalyst is apparent. A similar situation is observed in the case of Co_spongini. These results may be explained by the lower

Table 4. Calculated rate constants of 4-nitrophenol reduction over successive catalytic cycles

No. of cycle	Rate constant (min^{-1})		
	Co_spongin	Ag_spongin	Co-Ag_spongin
1	0.52	0.32	0.86
2	0.34	0.31	0.35
3	0.31	0.27	0.25
4	0.15	0.26	0.20
5	0.16	0.25	0.19

stability of the cobalt phase and blocking of the active sites of the catalyst over the reaction cycles. Interestingly, after the fifth run, the highest k parameter was calculated for Ag_spongin. For this material, the changes in the values of the rate constant are insignificant. This finding seems to be related to the chemical structure of spongin: the presence of free amide groups derived from cysteine and tyrosine led to better stability of the silver particles during the functionalization process. The results suggest that despite the high catalytic ability of Co_spongin, this material is the least stable, in view of the non-negligible decrease in the rate constant. Spongin modified with silver possesses higher stability; however, the rate of reduction is lower. Therefore, it may be assumed that the use of cobalt and silver together results in a material with higher catalytic ability and increased stability during reuse, in comparison to Co_spongin.

Further, to evaluate the changes in the morphology of the prepared materials after five catalytic cycles, SEM images of the used catalysts were recorded (Fig. 7).

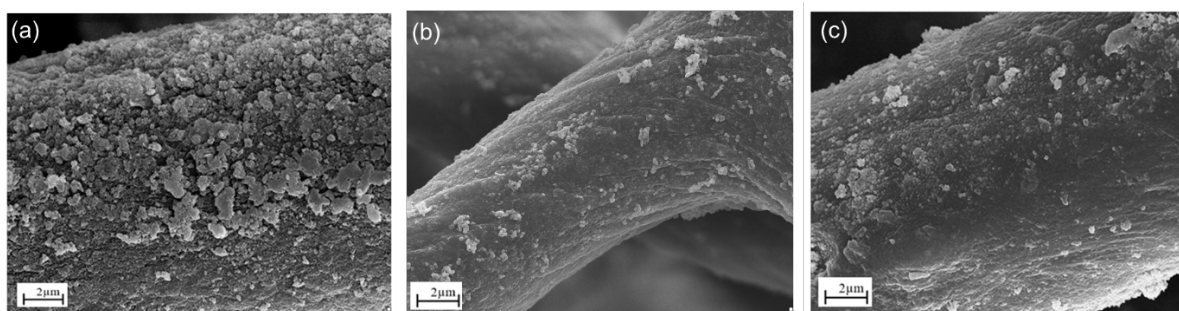


Fig. 7. SEM images of Co_spongin (a), Ag_spongin (b) and Co-Ag_spongin (c) used five times in catalytic cycles

From the images in Fig. 7 it is apparent that the structure and shape of the metallic phase do not change significantly after the catalytic tests. Moreover, the SEM images show that the size of the metallic grains remains unchanged after repeated reuse. The results provide evidence that spongin is a promising support for the metallic phase. The three-dimensional, fibrous structure of spongin, with a fascinating system of open-porous channels and a variety of functional groups, makes this material attractive for use in heterogeneous catalysis. The efficient functionalization method led to new composites which possess superior catalytic activity in the reduction of 4-nitrophenol. This study points a new direction for the development of heterogeneous catalysts based on spongin.

4. Conclusions

In conclusion, spongin of commercial sponge origin can be successfully applied as a support for cobalt/cobalt oxide, silver particles, as well as cobalt/cobalt oxide-silver particles. The facile functionalization method proposed in this work requires only the use of water solutions of cobalt and sodium salt, sodium borohydride as a reducer, and spongin skeleton. The naturally prefabricated, three-dimensional structure of spongin, with interconnected open-porous systems, provides excellent support for the metallic phase. The resulting composites are evenly covered with metallic particles,

which form agglomerates of different size and shape. EDS, TG/DTA and FTIR confirmed the successful synthesis of cobalt-based, silver-based and cobalt-silver-based composites. These materials exhibited good activity in the reduction of 4-nitrophenol to 4-aminophenol in water. The kinetic and reusability studies provide evidence that functionalization with both metallic phases results in composites with enhanced catalytic performance and good reusability properties, as well as significantly higher thermal stability. However, further work to explore the application of these composites, as well as the modification of synthesis methods, are important for the development of catalysts which might be utilized in other oxidation-reduction reactions. Nevertheless, spongin shows promise as a facile, cost-effective, renewable and environmentally friendly three-dimensional biopolymer for heterogeneous catalysis.

Dedication

The authors would like to dedicate this work to Professor Zygmunt Sadowski in gratitude for his constant inspiration, scientific discussion, and friendship.

Acknowledgements

The work was supported by the National Science Centre, Poland, project Etiuda no. 2019/32/T/ST8/00414, and by the Ministry of Science and Higher Education of Poland.

References

- AI, L., JING, J., 2013. *Catalytic reduction of 4-nitrophenol by silver nanoparticles stabilized on environmentally benign macroscopic biopolymer hydrogel*. *Bioresource Technol.* 132, 374–377.
- ALLAEDINI, G., ABUBAKAR, M., 2013. *Study of influential factors in synthesis and characterization of cobalt oxide nanoparticles*. *J. Nanostruct. Chem.* 3(77), 1–16.
- BOURY-ESNAULT, N., LAVROV, D.V., RUIZ, C.A., PÉREZ, T., 2013. *The integrative taxonomic approach applied to porifera: a case study of the Homoscleromorpha*. *Integr. Comp. Biol.* 53(3), 416–427.
- CHI, Y., WANG, M., LI, X., ZHANO, Z., 2014. *One-pot synthesis of ordered mesoporous silver nanoparticle/carbon composites for catalytic reduction of 4-nitrophenol*. *J. Colloid Interface Sci.* 423, 54–59.
- EHRlich, H., HANKE, T., MEISSNER, H., BORN, R., SCHARNWEBER, D., WORCH, H., 2003. *Spongins: nanostructural investigations and development of biomimetic material model*. *VDI Berichte* 1803, 287–290.
- GAO, Y., DING, X., ZHENG, Z., CHENG, X., PENG, Y., 2007. *Template-free method to prepare polymer nanocapsules embedded with noble metal nanoparticles*. *Chem. Comm.* 36, 3720–3722.
- GARCIA, E.M., SANTOS, J.S., PEREIRA, E.C., FREITAS, M.B.J.G., 2008. *Electrodeposition of cobalt from spent li-ion battery cathodes by the electrochemistry quartz crystal microbalance technique*. *J. Power Sources* 185(1), 549–553.
- GARRON, A., ŚWIERCZYŃSKI, D., BENNICI, S., AUROUX, A., 2009. *New insights into the mechanism of H₂ generation through NaBH₄ hydrolysis on Co-based nanocatalysts studied by differential reaction calorimetry*. *Int. J. Hydrog. Eng.* 34(3), 1185–1199.
- GREEN, D., HOWARD, D., YANG, X., KELLY, M., OREFFO, R.O.C., 2003. *Natural marine sponge fiber skeleton: a biomimetic scaffold for human osteoprogenitor cell attachment, growth, and differentiation*. *Tissue Eng.* 9(6), 1159–1166.
- GUO, J., WU, H., LIAO, X., SHI, B., 2011. *Facile synthesis of size-controlled silver nanoparticles using plant tannin grafted collagen fiber as reductant and stabilizer for microwave absorption application in the whole ku band*. *J. Phys. Chem. C* 115(48), 23688–23694.
- HANS, M., SALIMA, M., MÜCKLICH, F., SOLIOZ, M., 2016. *Physicochemical properties of copper important for its antibacterial activity and development of a unified model*. *Biointerphases* 11(1), 1–8.
- HUANG, X., WU, D., CHENG, D., 2017. *Porous Co₂P nanowires as high efficient bifunctional catalysts for 4-nitrophenol reduction and sodium borohydride hydrolysis*. *J. Colloid Interface Sci.* 507, 429–436.
- JESIONOWSKI, T., NORMAN, M., ŻÓŁTOWSKA-AKSAMITOWSKA, S., PETRENKO, I., JOSEPH, Y., EHRlich, H., 2018. *Marine spongin: naturally prefabricated 3D scaffold-based biomaterial*. *Mar. Drugs* 16(3), 1–23.
- KURODA, K., TAMAO, I., HARUTA, M., 2009. *Reduction of 4-nitrophenol to 4-aminophenol over Au nanoparticles deposited on PMMA*. *J. Mol. Catal. A Chem.* 298(1–2), 7–11.
- LIU, W., YANG, X., HUANG, W., 2006. *Catalytic properties of carboxylic acid functionalized-polymer microsphere-*

- stabilized gold metallic colloids. *J. Colloid Interface Sci.* 304(1), 160–165.
- LIU, W., YANG, X., XIE, L., 2007. Size-controlled gold nanocolloids on polymer microsphere-stabilizer via interaction between functional groups and gold nanocolloids. *J. Colloid Interface Sci.* 313(2), 494–502.
- MANDAL, A., MEDA, W., ZHANG, W.J., FARHAN, K.M., GNANAMANI, A., 2012. Synthesis, characterization and comparison of antimicrobial activity of PEG/TritonX-100 capped silver nanoparticles on collagen scaffold. *Colloids Surf B Biointerfaces* 90(1), 191–196.
- NOH, J., MEIJBOOM, R., 2014. Reduction of 4-nitrophenol as a model reaction for nanocatalysis. In *Application of Nanotechnology in Water Research*, ed. Mishra. AK., Scrivener Publishing LLC, Boston, USA.
- NORMAN, M., BARTCZAK, P., ZDARTA, J., EHRLICH, H., JESIONOWSKI, T., 2016b. Anthocyanin dye conjugated with *Hippospongia communis* marine demosponge skeleton and its antiradical activity. *Dyes Pigm.* 134, 541–552.
- NORMAN, M., ZDARTA, J., BARTCZAK, P., PIASECKI, A., PETRENKO, I., EHRLICH, H., JESIONOWSKI, T., 2016c. Marine sponge skeleton photosensitized by copper phthalocyanine: a catalyst for Rhodamine B degradation. *Open Chem.* 14(1), 243–254.
- NORMAN, M., BARTCZAK, P., ZDARTA, J., TOMALA, W., ŻURAŃSKA, B., DOBROWOLSKA, A., PIASECKI, A., CZACZYK, K., EHRLICH, H., JESIONOWSKI, T., 2016a. Sodium copper chlorophyllin immobilization onto *Hippospongia communis* marine demosponge skeleton and its antibacterial activity. *Int. J. Mol. Sci.* 17(10), 1564.
- NORMAN, M., ŻÓŁTOWSKA-AKSAMITOWSKA, S., ZGOŁA-GRZEŚKOWIAK, A., EHRLICH, H., JESIONOWSKI, T., 2018. Iron(III) phthalocyanine supported on a spongin scaffold as an advanced photocatalyst in a highly efficient removal process of halophenols and bisphenol A. *J. Hazard. Mater.* 347, 78–88.
- PALLELA, R., BOJJA, S., RAO, J.W., 2011. Biochemical and biophysical characterization of collagens of marine sponge, *Ircinia fusca* (Porifera: Demospongiae: Irciniidae). *Int. J. Biol. Macromol.* 49(1), 85–92.
- PETRENKO, I., SUMMERS, A.P., SIMON, P., ŻÓŁTOWSKA-AKSAMITOWSKA, S., MOTYLENKO, M., SCHIMPF, K., RAFAJA, D., ROTH, F., KUMMER, K., BRENDLER, E., POKROVSKY, P.S., GALLI, R., WYSOKOWSKI, M., MEISSNER, H., NIEDERSCHLAG, E., JOSEPH, Y., MOLODTSOV, S., ERESKOVSKY, A., SIVKOV, V., NEKIPELOV, S., PETROVA, O., VOLKOVA, O., BERTAU, M., KRAFT, M., ROGALEV, A., KOPANI, M., JESIONOWSKI, T., EHRLICH, H., 2019. Extreme Biomimetics: preservation of molecular detail in centimeter-scale samples of biological meshes laid down by sponges. *Sci. Adv.* 5(10), 1–12.
- PICH, A., KARAK, A., LU, Y., GHOSH, A.K., ADLER, H.-J.P., 2006. Tuneable catalytic properties of hybrid microgels containing gold nanoparticles. *J. Nanosci. Nanotechnol.* 6(12), 3763–3769.
- SHARMA, A., DUTTA, R.K., ROYCHOWDHURY, A., DAS, D., GOYAL, A., KAPOOR, A., 2017. Cobalt doped CuO nanoparticles as a highly efficient heterogeneous catalyst for reduction of 4-nitrophenol to 4-aminophenol. *Appl. Catal. A Gen.* 543, 257–265.
- SZATKOWSKI, T., JESIONOWSKI, T., 2017. Hydrothermal synthesis of spongin-based materials. In *Extreme Biomimetics*, ed. Ehrlich, H., Springer Nature, Cham, Switzerland, 251–274.
- SZATKOWSKI, T., WYSOKOWSKI, M., LOTA, G., PEŹIAK, D., BAZHENOV, V.V., NOWACZYK, G., WALTER, J., MOLODTSOV, S.L., STOCKER, H., HIMCINSCHI, C., PETRENKO, I., STELLING, A.L., JURGA, S., JESIONOWSKI, T., EHRLICH, H., 2015. Novel nanostructured hematite–spongin composite developed using an Extreme Biomimetic approach. *RSC Adv.* 5(96), 79031–79040.
- SZATKOWSKI, T., SIWIŃSKA-STEFAŃSKA, K., WYSOKOWSKI, M., STELLING, A.L., JOSEPH, Y., EHRLICH, H., JESIONOWSKI, T., 2017. Immobilization of titanium(IV) oxide onto 3D spongin scaffolds of marine sponge origin according to Extreme Biomimetics principles for removal of C.I. Basic Blue 9. *Biomimetics* 2(2), 1–14.
- SZATKOWSKI, T., KOPCZYŃSKI, K., MOTYLENKO, M., BORMANN, H., MANIA, B., GRAŚ, M., LOTA, G., BAZHENOV, V.V., RAFAJA, D., ROTH, D., WEISE, J., LANGER, E., WYSOKOWSKI, M., ŻÓŁTOWSKA-AKSAMITOWSKA, S., PETRENKO, I., MOLODTSOV, S.L., HUBALKOVA, J., ANEZIRIS, C.G., JOSEPH, Y., STELLING, A.L., EHRLICH, H., JESIONOWSKI, T., 2018. Extreme Biomimetics: a carbonized 3D spongin scaffold as a novel support for nanostructured manganese oxide(IV) and its electrochemical applications. *Nano Res.* 11(8), 4199–4214.
- WU, H., HUANG, X., GAO, M., LIAO, X., SHI, B., 2011. Polyphenol-grafted collagen fiber as reductant and stabilizer for one-step synthesis of size-controlled gold nanoparticles and their catalytic application to 4-nitrophenol reduction. *Green Chem.* 13(3), 651–658.
- ZDARTA, J., NORMAN, M., SMUŁEK, W., MOSZYŃSKI, D., KACZOREK, E., STELLING, A.L., EHRLICH, H., JESIONOWSKI, T., 2017. Spongin-based scaffolds from *Hippospongia communis* demosponge as an effective support for lipase immobilization. *Catalysts* 7(5), 147, 1–20.